AIAA/AAS Astrodynamics Specialist Conference and Exhibit
5-8 August 2002, Monterey, California

AIAA 2002-4



# ATTITUDE DYNAMICS OF SATELLITES ORBITING SMALL BODIES

Jean-Luc Riverin and Arun K. Misra
Department of Mechanical Engineering
McGill University
Montreal, QC, Canada H3A 2K6



## ABSTRACT

Attitude motion of satellites orbiting a small body (such as an asteroid or a comet) is examined. The highly irregular shape of the small bodies along with their rotational states can lead to very interesting attitude dynamics. As a start, the case of uniform rotation of the small body is examined and attention is focused on planar attitude motion (pitch). Four asteroids, Vesta, Eros, Gaspra and Castalia, are considered. For the case of circular equatorial orbits, the radius for which resonant pitch oscillations are excited, is determined. It is noticed that for slowly rotating large asteroids such as Vesta, more than one resonant region can exist. Stability of pitch motion is significantly affected by the rotational state as well as the shape of the small body. Analysis for elliptic orbits indicates that motion that is stable for circular orbits can be destabilized for a small eccentricity.

## INTRODUCTION

A small body is a celestial object that has a mean diameter of less than 1000 km. This includes mainly asteroids and comets. The largest asteroid, 1 Ceres, has a diameter of approximately 940 km.[1] Small bodies are studied by scientists because of the insight they can give about the history of the solar system.

Interest in spacecraft missions to small bodies has increased in recent years. The NEAR-Shoemaker mission to 433 Eros was a very successful one. After observing the asteroid for a few months, the spacecraft eventually landed on it in February 2001. Several other missions to asteroids and comets are currently under development. One of the key elements in designing such a mission is the analysis of the dynamical behavior of the spacecraft in the vicinity of the small body. Both orbital and attitude dynamics can be quite complex and sometimes very different from that around a large body such as the Earth.

Several papers have addressed the problem of orbital dynamics about small bodies. The irregular shape, mass distribution as well as the state of rotation of the small body, have significant effects on the evolution of the orbit of the spacecraft.

Probably the first paper to address specifically the problem of orbital dynamics about small bodies is one by Chauvineau and Mignard[2], in which the possibility of putting an artificial satellite in orbit about a strongly non-spherical asteroid was assessed. The primary body was assumed to be a homogeneous tri-axial ellipsoid rotating uniformly about its shortest axis. The results were obtained for orbits restricted to lie in the equatorial plane. It was noticed that a chaotic region appears close to the 1:1 resonance between the asteroid's rotation period and the orbital period of the satellite.

Scheeres and his co-workers have made a large number of contributions to the study of orbital motion about asteroids. Scheeres[3,4] presented a complete formulation of the problem of orbital dynamics about uniformly rotating asteroids. He showed that small bodies can be classified into two different types that describe qualitatively the stability of near-synchronous orbits. Scheeres[5] and Scheeres et al.[6,7] also considered orbital dynamics specifically about asteroids Eros, Castalia and Toutatis, respectively. The last of the above papers investigated close-orbit motion about an irregularly shaped body in a state of non-principal-axis rotation. It was emphasized that the state of rotation of the asteroid has significant impact on osculating orbital elements, and the resulting orbits are quite complex.

Dynamical issues associated with hovering[8] and landing[9] on an asteroid have also been examined, however attitude dynamics of a satellite orbiting a small body have not been studied. Attitude dynamics in this case can be as interesting as orbital dynamics, for the same reasons. The objective of the present paper is to study this attitude dynamics.

## EQUATIONS OF MOTION

The scenario considered in this paper is similar to the one examined by Chavineau and Mignard[2] for orbital

motion. The following assumptions are made in deriving the equations of motion.

(i) The rotation rate of the primary body is constant;

(ii) Orbital motion of the spacecraft is fully described as a closed, planar and periodic orbit;

(iii) Orbital motion of the spacecraft is affected negligibly by attitude dynamics;

(iv) The only external force acting on the spacecraft is the gravitational attraction of the small primary body;

(v) The spacecraft is rigid.

In view of the last assumption, the attitude motion can be described by Euler's equations of motion for a rigid body:

$$I_1\dot{\omega}_1 - (I_2 - I_3)\omega_2\omega_3 = M_1, \quad (1)$$

$$I_2\dot{\omega}_2 - (I_3 - I_1)\omega_3\omega_1 = M_2, \quad (2)$$

$$I_3\dot{\omega}_3 - (I_1 - I_2)\omega_1\omega_2 = M_3, \quad (3)$$

where $I_1, I_2, I_3$ are the principal moments of inertia of the spacecraft, $\omega_1, \omega_2, \omega_3$ are the components of the angular velocity along the principal axes, while $M_1, M_2, M_3$ are the components of the external moment, in this case caused solely by the gravitational field of the asteroid.

For further development of equations (1)–(3), it is convenient to define the following co-ordinate frames. A set of three orthogonal unit vectors (**I, J, K**) is fixed to the center of mass of the asteroid. These axes are assumed to be inertial. Another set of unit vectors $(\mathbf{I}', \mathbf{J}', \mathbf{K}')$ is fixed to the asteroid such that the vectors are aligned along the three centroidal principal axes of smallest, intermediate and largest moment of inertia, respectively. The asteroid rotational state relates the two frames (**I, J, K**) and $(\mathbf{I}', \mathbf{J}', \mathbf{K}')$. A third frame, the orbital frame, consists of three orthogonal unit vectors ($\mathbf{0}_1$, $\mathbf{0}_2$, $\mathbf{0}_3$) defined such that $\mathbf{0}_3$ points towards the center of mass of the asteroid, $\mathbf{0}_1$ is in the transverse direction in the orbital plane, and $\mathbf{0}_2 = \mathbf{0}_3 \times \mathbf{0}_1$, according to the right hand rule (Figure 1). For equatorial orbits, the orbital frame is obtained from the inertial frame (**I, J, K**) by a single rotation through an angle equal to the true anomaly $\eta$. Finally, the unit vectors ($\mathbf{b}_1$, $\mathbf{b}_2$, $\mathbf{b}_3$) are defined along the principal axes of the spacecraft. Their orientation with respect to the orbital frame can be defined in terms of the roll, pitch and yaw angles. The sequence of rotations used here is: yaw $(\theta_3)$, followed by pitch $(\theta_2)$, which is then followed by roll $(\theta_1)$. Hence, the angular velocity components appearing in eqs. (1)–(3) are given by

$$\begin{bmatrix}\omega_1\\ \omega_2\\ \omega_3\end{bmatrix} = \begin{bmatrix}1 & 0 & -\sin\theta_2\\ 0 & \cos\theta_1 & \sin\theta_1\cos\theta_2\\ 0 & -\sin\theta_1 & \cos\theta_1\cos\theta_2\end{bmatrix}\begin{bmatrix}\dot{\theta}_1\\ \dot{\theta}_2\\ \dot{\theta}_3\end{bmatrix} - \begin{bmatrix}\cos\theta_2\sin\theta_3\\ \sin\theta_1\sin\theta_2\sin\theta_3 + \cos\theta_1\cos\theta_3\\ \cos\theta_1\sin\theta_2\sin\theta_3 - \sin\theta_1\cos\theta_3\end{bmatrix}\dot{\eta} \quad (4)$$

where $\dot{\eta}$ is the instantaneous orbital rate.

**Gravity-gradient Torques**: As mentioned earlier, the only external force acting on the spacecraft is the gravitational attraction of the small body. The gravitational potential of any arbitrary primary can be written in the form[7]

$$U = \frac{\mu}{R}\left[1 + \frac{1}{2}\left(\frac{r_0}{R}\right)^2 C_{20}\left(3\sin^2\delta - 1\right) + 3\left(\frac{r_0}{R}\right)^2 C_{22}\cos^2\delta\cos(2\lambda) + \frac{1}{2}\left(\frac{r_0}{R}\right)^3 C_{30}\sin\delta\left(5\sin^2\delta - 3\right) + \ldots\right], \quad (5)$$

where $R$ is the distance of an orbiting particle from the center of mass of the primary, $r_0$ is the characteristic length of the primary, while $\delta$ and $\lambda$ are respectively the latitude and longitude of the orbiting particle measured in an asteroid-fixed frame. The terms $C_{20}$, $C_{22}$, $C_{30}$… are gravitational coefficients that are specific to a given shape. The terms $C_{20}$, $C_{30}$,… characterize the oblateness of a body, where the coefficients $C_{22}$,…, characterize the ellipticity of its equator. For the Earth, $C_{20}$ is $O(10^{-3})$ and the other coefficients are $O(10^{-6})$; however, for some familiar asteroids these coefficients can be as high as $0.9\times10^{-1}$. Thus the non-spherical shape of an asteroid can have a much stronger effect on both orbital and attitude dynamics. Table 1 shows the values of $r_0, C_{20}$ and $C_{22}$ for some asteroids (extracted from References 4-6). The gravitational

force acting on a particle of mass $dm$ at a distance $R$ from the asteroid center of mass, having latitude $\delta$ and longitude $\lambda$, is given by

$$d\mathbf{F} = \left[ \frac{\partial U}{\partial R}\mathbf{e_R} + \frac{1}{R\cos\delta}\frac{\partial U}{\partial \lambda}\mathbf{e_\lambda} + \frac{1}{R}\frac{\partial U}{\partial \delta}\mathbf{e_\delta} \right] dm, \quad (6)$$

where U is as given in eq. (5), while $\mathbf{e_R}, \mathbf{e_\lambda}, \mathbf{e_\delta}$ are unit vectors associated with the spherical coordinate system R, $\lambda, \delta$. The position vector $\mathbf{R}$ of the element can be expressed as

$$\mathbf{R} = \mathbf{R_C} + \mathbf{r} \quad (7)$$

Table 1: Gravitational Coefficients of Second Order for Some Asteroids

| Asteroid | $r_0$(km) | $C_{20}$ | $C_{22}$ |
|---|---|---|---|
| Vesta | $2.443 \times 10^2$ | 0.0512 | -0.0055 |
| Castalia | $5.429 \times 10^{-1}$ | -0.0891 | 0.0305 |
| Eros | $9.933 \times 10^0$ | -0.0878 | 0.0439 |
| Ida | $1.522 \times 10^1$ | -0.0902 | 0.0408 |
| Gaspra | $6.793 \times 10^0$ | -0.0729 | 0.0301 |

where $\mathbf{R_C}$ is the position vector of the center of mass of the spacecraft relative to the asteroid center of mass, while $\mathbf{r}$ is the position vector of the element in the spacecraft frame. Clearly,

$$\mathbf{R} = |\mathbf{R_C} + \mathbf{r}|, \quad \mathbf{e_R} = \frac{\mathbf{R_C} + \mathbf{r}}{|\mathbf{R_C} + \mathbf{r}|}, \quad \mathbf{e_\lambda} = \mathbf{e_\delta} \times \mathbf{e_R}. \quad (8)$$

Substituting eqs. (5), (7) and (8) into eq. (6), one obtains

$$d\mathbf{F} = d\mathbf{F_R} + d\mathbf{F}_\lambda + d\mathbf{F}_\delta, \quad (9)$$

where

$$d\mathbf{F_R} = -\frac{\mu dm(\mathbf{R_C} + \mathbf{r})}{|\mathbf{R_C} + \mathbf{r}|^3}\left[ 1 + \frac{3}{2}\left( \frac{r_0}{|\mathbf{R_C} + \mathbf{r}|} \right)^2 C_{20}\left( 3\sin^2\delta - 1 \right) \right.$$

$$+ 9\left( \frac{r_0}{|\mathbf{R_C} + \mathbf{r}|} \right)^2 C_{22}\cos^2\delta\cos(2\lambda)$$

$$\left. + 2\left( \frac{r_0}{|\mathbf{R_C} + \mathbf{r}|} \right)^3 C_{30}\sin\delta\left( 5\sin^2\delta - 3 \right) \right], \quad (10)$$

$$d\mathbf{F_\lambda} = -\frac{\mu dm[\mathbf{e_\delta} \times (\mathbf{R_C} + \mathbf{r})]}{|\mathbf{R_C} + \mathbf{r}|^3}$$

$$\left[ 6\left( \frac{r_0}{|\mathbf{R_C} + \mathbf{r}|} \right)^2 C_{22}\cos\delta\sin(2\lambda) \right], \quad (11)$$

$$d\mathbf{F_\delta} = \frac{\mu dm\mathbf{e_\delta}}{|\mathbf{R_C} + \mathbf{r}|^2}\left[ 3\left( \frac{r_0}{|\mathbf{R_C} + \mathbf{r}|} \right)^2 C_{20}\sin\delta\cos\delta \right.$$

$$- 6\left( \frac{r_0}{|\mathbf{R_C} + \mathbf{r}|} \right)^2 C_{22}\sin\delta\cos\delta\cos(2\lambda)$$

$$\left. + \frac{3}{2}\left( \frac{r_0}{|\mathbf{R_C} + \mathbf{r}|} \right)^3 C_{30}\left( 5\sin^2\delta - 1 \right)\cos\delta \right]. \quad (12)$$

The gravity gradient torque on the spacecraft can then be determined from

$$\mathbf{M} = \int \mathbf{r} \times d\mathbf{F}. \quad (13)$$

Evaluation of this torque involves expansion of the various powers of $|(\mathbf{R_C} + \mathbf{r})|$ using the binomial theorem, and neglecting terms involving third and higher powers of $|\mathbf{r}|/|\mathbf{R_C}|$.

**Planar Attitude Motion for Equatorial Orbits.** Consider now the case of a satellite in an equatorial orbit undergoing planar pitch motion. It is also assumed that the asteroid is rotating with a constant angular velocity $\Omega\mathbf{K}$. The longitude of the center of mass of the satellite is then given by

$$\lambda_c = \eta \pm \Omega t, \quad (14)$$

where the plus and minus signs apply for retrograde and direct orbits, respectively. For circular orbits, $\dot{\eta} = n = \text{constant}$ and $\lambda_c$ is given by

$$\lambda_c = (n \pm \Omega)t, \quad (15)$$

where $n$ is the orbital angular velocity of the spacecraft. Evaluation of the gravity gradient torque using eq. (13) yields, after some algebra,

$$M_1 = M_3 = 0, \quad (16)$$

$$M_2 = \frac{\mu}{R_C^3} I_2 \left[ -(3+5\varphi) k_2 \sin\theta_2 \cos\theta_2 \right.$$

$$\left. + \frac{1}{2}\chi \left\{ 3 + 5k_2 \left( \cos^2\theta_2 - \sin^2\theta_2 \right) \right\} \right], \qquad (17)$$

where $k_2$ is the inertia ratio $(I_1 - I_3)/I_2$, and

$$\varphi = \left[ -\frac{3}{2} C_{20} + 9 C_{22} \cos(2\lambda_c) \right] \left( \frac{r_0}{R_C} \right)^2, \qquad (18)$$

$$\chi = \left[ 6 C_{22} \sin(2\lambda_c) \right] \left( \frac{r_0}{R_C} \right)^2. \qquad (19)$$

Only one equation of motion, eq. (2), exists for the planar case, which with the use of eqs. (4) and (15) becomes

$$\ddot{\theta}_2 + \frac{\mu}{R_C^3}(3+5\varphi) k_2 \sin\theta_2 \cos\theta_2$$

$$- \frac{1}{2}\frac{\mu}{R_C^3}\chi \left\{ 3 + 5k_2 \left( \cos^2\theta_2 - \sin^2\theta_2 \right) \right\} - \ddot{\eta} = 0 . \qquad (20)$$

**Three-Dimensional Small Motion for Equatorial Orbits**: A satellite in an equatorial orbit is considered again, but now the attitude motion is allowed to be three-dimensional but small. The asteroid is again assumed to have a constant angular velocity $\Omega\mathbf{K}$. The unit vectors $\mathbf{e_R}$, etc. appearing in eqs. (8), (10)–(12) can now be expressed in terms of the yaw, pitch, and roll angles. The gravity gradient torque components, for small motion, then become

$$M_1 = \frac{\mu}{R_C^3} I_1 \left[ -(3+5\varphi) k_1 \theta_1 + \frac{1}{2}\chi (3+5k_1)\theta_3 \right], \qquad (21)$$

$$M_2 = \frac{\mu}{R_C^3} I_2 \left[ -(3+5\varphi) k_2 \theta_2 + \frac{1}{2}\chi (3+5k_2) \right], \qquad (22)$$

$$M_3 = \frac{\mu}{R_C^3} I_3 \left[ -\frac{1}{2}\chi (3-5k_3)\theta_1 \right], \qquad (23)$$

where $k_2$ is as defined earlier, while $k_1, k_3$ are inertia ratios given by $(I_2 - I_3)/I_1$ and $(I_2 - I_1)/I_3$, respectively. Furthermore, for small motion, the angular velocity components given in eq. (4) become

$$\begin{bmatrix} \omega_1 \\ \omega_2 \\ \omega_3 \end{bmatrix} = \begin{bmatrix} \dot{\theta}_1 - \dot{\eta}\theta_3 \\ \dot{\theta}_2 - \dot{\eta} \\ \dot{\theta}_3 + \dot{\eta}\theta_1 \end{bmatrix} \qquad (24)$$

Introducing eqs. (21)–(24) into eqs. (1)–(3), one obtains the equations of motion

$$\ddot{\theta} + \dot{\eta}(k_1 - 1)\dot{\theta}_3 + \left[ \frac{\mu}{R_C^3}(3+5\varphi) + \dot{\eta}^2 \right] k_1 \theta_1$$

$$- \left[ \frac{1}{2}\frac{\mu}{R_C^3}\chi (3+5k_1) + \ddot{\eta} \right] \theta_3 = 0 , \qquad (25)$$

$$\ddot{\theta}_2 - \ddot{\eta} + \frac{\mu}{R_C^3}(3+5\varphi)\, k_2\theta_2 - \frac{1}{2}\frac{\mu}{R_C^3}\chi (3+5k_2) = 0 , \qquad (26)$$

$$\ddot{\theta}_3 + \dot{\eta}(1-k_3)\dot{\theta}_1 + \left[ \ddot{\eta} + \frac{1}{2}\frac{\mu}{R_C^3}\chi (3-5k_3) \right] \theta_1$$

$$+ k_3 \dot{\eta}^2 \theta_3 = 0 . \qquad (27)$$

## ANALYSIS OF PLANAR MOTION IN CIRCULAR ORBITS

For circular orbits, $\dot{\eta} = n = \text{const.}$, $\ddot{\eta} = 0$, $\mu / R_C^3 = n^2$. Equation (20) then reduces to

$$\ddot{\theta}_2 + n^2 (3+5\varphi) k_2 \sin\theta_2 \cos\theta_2$$

$$- \frac{1}{2} n^2 \chi \left[ 3 + 5k_2 \cos(2\theta_2) \right] = 0 , \qquad (28)$$

and the longitude $\lambda_c$ appearing in $\varphi$ and $\chi$ is given by eq. (15). To obtain an understanding of the pitch behavior, let us consider small motion. Equation (28) then reduces to

$$\ddot{\theta}_2 + n^2 (3+5\varphi) k_2 \theta_2 - \frac{1}{2} n^2 \chi (3+5k_2) = 0. \qquad (29)$$

The quantities $\varphi$ and $\chi$ are periodic as can be seen from eqs. (18), (19) and (15). One can cast eq. (29) in the form

$$\ddot{\theta}_2 + (A + B\cos\nu t)\theta_2 = D\sin\nu t \tag{30}$$

$$A = \left[3 - \frac{15}{2}C_{20}\left(\frac{r_0}{R_C}\right)^2\right] n^2 k_2, \tag{31}$$

$$B = 45\,C_{22}\left(\frac{r_0}{R_C}\right)^2 n^2 k_2, \tag{32}$$

$$C = 3\,C_{22}\left(\frac{r_0}{R_C}\right)^2 n^2 (3 + 5k_2), \tag{33}$$

$$\nu = 2(n \pm \Omega). \tag{34}$$

The plus and minus signs hold for retrograde and direct orbits, respectively. If $k_2$ is negative, the pitch motion is normally unstable; hence the case of positive $k_2$ is considered mostly in this paper. It should also be noted that normally $B$ is less than $A$.

Equation (30) represents a harmonically excited system with periodic stiffness. There are two situations when large pitch motion can result. One is the case of resonance when $\nu$ is equal to $\sqrt{A}$. The other is parametric resonance; one can notice that eq. (30) can be converted to a forced Mathieu equation.

Regular resonance takes place when $\nu = \pm\sqrt{A}$, or

$$2(n \pm \Omega) = \pm\left[\left\{3 - \frac{15}{2}C_{20}\left(\frac{r_0}{R_C}\right)^2\right\} k_2\right]^{1/2} n. \tag{35}$$

Since $k_2 < 1$ and $|C_{20}| < 0.1$, eq. (35) cannot be satisfied with the plus sign on the LHS. Choosing the minus sign in the LHS in eq. (35), resonance occurs when the asteroid and orbital angular velocities are related by

$$\frac{\Omega}{n} = 1 \mp \frac{(3k_2)^{1/2}}{2}\left\{1 - \frac{5}{2}C_{20}\left(\frac{r_0}{R_C}\right)^2\right\}^{1/2}, \tag{36}$$

or approximately,

$$\frac{\Omega}{n} \approx 1 \mp \frac{(3k_2)^{1/2}}{2}. \tag{37}$$

Table 2: Orbit radius for pitch resonance

| Asteroid | Resonant Orbit Radius | | | | | |
|---|---|---|---|---|---|---|
| | $k_2 = 1/3$ | | $k_2 = 1/2$ | | $k_2 = 2/3$ | |
| | km | Nondim. | km | Nondim. | km | Nondim. |
| Vesta | 667.56<br>312.04 | 2.73<br>1.28 | 700.56 | 2.87 | 727.74 | 2.98 |
| Gaspra | 22.35<br>10.46 | 3.32<br>1.55 | 23.45 | 3.48 | 24.36 | 3.61 |
| Eros | 26.29 | 2.65 | 27.59 | 2.78 | 28.66 | 2.89 |
| Castalia | 1.05 | 1.94 | 1.11 | 2.04 | 1.15 | 2.12 |

Two pitch-resonant orbits (corresponding to both signs in eq. (36)) can be found for massive, compact and/or slowly rotating asteroids if $k_2$ is small enough. Table 2 presents resonant orbital radius for some common asteroids. The radius is shown in km as well as in the nondimensional form after division by $r_o$, the mean radius of the asteroid. Numerical results showing the resonance effect are presented in the next section.

The equation of motion, eq. (30), can be rewritten as

$$\frac{d^2\theta_2}{dz^2} + (a + 2b\cos 2z)\theta_2 = d\sin 2z, \tag{38}$$

where

$$z = \frac{1}{2}\nu t, \quad a = \left(4/\nu^2\right)A, \quad b = \left(4/\nu^2\right)B, \quad d = \left(4/\nu^2\right)D. \tag{39}$$

Equation (38) is the forced Mathieu equation. The homogeneous solution of eq. (38) is unstable when $a$ is close to the square of an integer[10], i.e.,

$$a = m^2, \quad m = 1, 2, 3, \ldots \text{ or}$$

$$\frac{3n^2}{(n \pm \Omega)^2}\left[1 - \frac{5}{2}C_{20}\left(\frac{r_0}{R_C}\right)^2\right] k_2 = m^2. \tag{40}$$

The second term inside the square bracket in eq. (40) is normally much smaller than 1; hence the parametric resonance condition can be approximated as

$$\frac{\Omega}{n} = \frac{m \mp (3k_2)^{1/2}}{m}, \quad m = 1, 2, 3, \ldots \tag{41}$$

It may be noted that for $m = 2$, eq. (41) reduces to eq. (37), the condition for standard resonance. Tables 3 and 4 present the orbit radius leading to parametric resonance for some common asteroids, for $m = 1$ and

$m = 3$, respectively. The case of $m = 2$ is represented by Table 2.

Table 3: Orbit radius for pitch internal resonance, $m = 1$.

| Asteroid | Resonant Orbit Radius | | | | | |
|---|---|---|---|---|---|---|
| | $k_2$ = 1/3 | | $k_2$ = 1/2 | | $k_2$ = 2/3 | |
| | Km | Nondim. | Km | Nondim. | Km | Nondim. |
| Vesta | 808.73 | 3.31 | 868.14 | 3.55 | 916.70 | 3.75 |
| Gaspra | 27.07 | 4.02 | 29.07 | 4.31 | 30.69 | 4.55 |
| Eros | 31.85 | 3.21 | 34.19 | 3.44 | 36.10 | 3.63 |
| Castalia | 1.28 | 2.35 | 1.37 | 2.53 | 1.45 | 2.67 |

Table 4: Orbit radius for pitch internal resonance, $m = 3$

| Asteroid | Resonant Orbit Radius | | | | | |
|---|---|---|---|---|---|---|
| | $k_2$ = 1/3 | | $k_2$ = 1/2 | | $k_2$ = 2/3 | |
| | Km | Nondim. | Km | Nondim. | Km | Nondim. |
| Vesta | 576.19<br>359.41 | 2.36<br>1.47 | 639.99<br>353.42 | 2.62<br>1.45 | 659.03<br>325.38 | 2.70<br>1.33 |
| Gaspra | 20.66<br>12.88 | 3.06<br>1.91 | 21.43<br>11.84 | 3.18<br>1.76 | 22.06<br>10.90 | 3.27<br>1.62 |
| Eros | 24.29 | 2.45 | 25.20 | 2.54 | 25.95 | 2.61 |
| Castalia | 0.97 | 1.79 | 1.01 | 1.86 | 1.04 | 1.92 |

## NUMERICAL RESULTS FOR THE PLANAR CASE

Equation (20) was solved numerically using a multi-step, predictor-corrector solver in Matlab, based on the Adams-Bashforth-Moulton algorithm with absolute and relative tolerances of $1\times10^{-10}$. All the results were obtained using the initial conditions $\theta_2(0) = 0.1$ rad, $\dot{\theta}_2(0) = 0$.

Figure 2 shows the pitch motion of a satellite with $k_2 = 1/3$ in an equatorial circular orbit about Eros at $R_C = 50$ km, comparable to the altitude where the spacecraft NEAR has been placed. The pitch motion is quite regular with amplitude of 0.1 rad. Figure 3 shows the pitch motion when $R_C = 32$ km. Parametric pitch resonance at $m = 1$ is supposed to occur approximately at this altitude, but it does not seem to be very pronounced. Pitch motions for $R_C = 26$ and 25.3 km are shown in Figures 4 and 5, respectively. One can notice large resonant oscillations. Linear analysis predicts resonance at $R_C = 26.29$ km (Table 2) and $m = 3$ parametric resonance at 24.29 km (Table 4), but in nonlinear simulation the resonances occur at slightly different radius. When $R_C$ is reduced further to 20 km, pitch motion becomes small again, with amplitude of 0.1 rad, approximately. Figures 6-8 present pitch motion of a satellite about Castalia at $R_C = 2$, 1.05 and 1.03 km, respectively. The motion is small at 2 km radius, shows resonance at 1.05 km and becomes unstable at $R_C = 1.03$ km. Figures 9-11 show similar pitch oscillations of a satellite about Vesta. At $R_C = 500$ km, the motion is small (Figure 9), but at $R_C = 661$ and 312 km, there are large resonant motions as shown in Figures 10 and 11, respectively. These are the two resonant radii for Vesta for $k_2 = 1/3$, as shown in Table 2.

## PITCH MOTION IN ELLIPTIC ORBITS

The previous discussion on circular orbits allowed to shed some light on some interesting dynamical features associated with attitude motion in a circular orbit about an asteroid. This section presents an initial attempt at analysis of pitch motion in an elliptic orbit about an asteroid. The radius $R_C$ and true anomaly $\eta$ are related by

$$R_C = \frac{a\left(1-e^2\right)}{1+e\cos\eta}, \tag{42}$$

where $e$ is the eccentricity. The true anomaly rate is then given by

$$\dot{\eta} = n\left(1-e^2\right)^{-3/2}\left(1+e\cos\eta\right)^2, \tag{43}$$

where $n$ is the mean orbital rate. A change of the independent variable from $t$ to $\eta$ transforms eq. (20) to

$$\left(1+e\cos\eta\right)\frac{d^2\theta_2}{d\eta^2} - 2e\sin\eta\,\frac{d\theta_2}{d\eta}$$

$$+\left(3+5\varphi\right)k_2\sin\theta_2\cos\theta_2$$

$$\equiv 2e\sin\eta + \frac{1}{2}\chi\left\{3+5k_2\cos 2\theta_2\right\}, \tag{44}$$

where $\phi$ and $\chi$ are functions of $\eta$. Defining

$$z = \left(1+e\cos\eta\right)\theta_2, \tag{45}$$

and assuming small eccentricity, one can obtain

$$\frac{d^2z}{d\eta^2} + \left[\left(3+5\hat{\varphi}\right)k_2 + \left\{1-\left(3+5\hat{\varphi}\right)k_2\right\}e\cos\eta\right]z = f\left(\eta\right), \tag{46}$$

where

$$\hat{\varphi} = \left[-\frac{3}{2}C_{20} + 9C_{22}\cos 2\lambda_c\right]\left(\frac{r_0}{a}\right)^2. \tag{47}$$

Equation (46) is a forced Mathieu equation and the homogeneous solution has parametric resonance near

$$4\left(3+5\hat{\varphi}\right)k_2 = m, \quad m = 1,2,3\ldots \tag{48}$$

Thus the critical values for $k_2$ are $\frac{1/12}{1+\frac{5}{3}\hat{\varphi}}$, $\frac{1/3}{1+\frac{5}{3}\hat{\varphi}}$, $\frac{3/4}{1+\frac{5}{3}\hat{\varphi}}$. If the spacecraft is sufficiently far from the asteroid, $\hat{\varphi}$ is small and critical values of $k_2$ are 1/12, 1/3, 3/4. It may be recalled that for geocentric satellites, $k_2 = 1/3$ leads to resonance.

## CONCLUSIONS

The paper attempts to obtain an understanding of the attitude motion of a spacecraft orbiting a small body. It appears that the nonspherical shape and the rotational state of asteroids can have important effects on pitch motion. Several familiar asteroids are considered and radii of circular orbits at which resonance or parametric resonance occurs, are determined. Numerical simulations using the nonlinear equation confirm the analytical results. Inertia parameters for which parametric resonance occurs in elliptic orbits, are determined.

## ACKNOWLEDGEMENTS

The research work reported in this paper was partially supported by the natural Sciences and Engineering Research Council of Canada. The authors gratefully acknowledge the computational work carried out by Mr. Philippe Chaput.

## REFERENCES

1. Kowal, C.T., *Asteroids: Their Nature and Utilization*, Wiley & Praxis, Chichester, UK, 1996.
2. Chauvineau, B. and Mignard, F., "Planar Orbits about a Triaxial Body: Application to Asteroidal Satellites", *Icarus*, Vol. 105, 1993, pp. 370-384.
3. Scheeres, D.J., "Dynamics about Uniformly Rotating Triaxial Ellisoids: Applications to Asteroids", *Icarus*, Vol. 110, 1994, pp. 225-238.
4. Scheeres, D.J., "Satellite Dynamics about Asteroids", *Spaceflight Mechanics*, Vol. 37, 1994, pp. 275-292.
5. Scheeres, D.J., "Analysis of Orbital Motion Around 433 Eros", *The Journal of Astronautical Sciences*, Vol. 43, 1995, pp. 427-452.
6. Scheeres, D.J., Ostro, S.J., Hudson, R.S. and Werner, R.A., "Orbits Close to Asteroid 4769 Castalia", *Icarus*, Vol. 121, 1996, pp. 67-87.
7. Scheeres, D.J., Ostro, S.J., Hudson, R.S., DeJong, E.M. and Suzuki, S., "Dynamics of Orbits Close to Asteroid 4179 Toutatis", *Icarus*, Vol. 132, 1998, pp. 53-79.
8. Sawai, S. and Scheeres, D.J., "Hovering and Translational Motions over Small Bodies", *AAS/AIAA Space Flight Mechanics Meeting*, Santa Barbara, California, February 2001, Paper No. AAS-01-157.
9. Scheeres, D.J., "Design and Analysis of Landing and Low-Altitude Asteroid Flyovers", *AAS/AIAA Space Flight Mechanics Meeting*, Santa Barbara, California, February 2001, Paper No. AAS-01-138.
10. Nayfey, A.H. and Mook, D.T., *Nonlinear Oscillations*, John Wiley & Sons, New York, 1979, pp. 258-299.

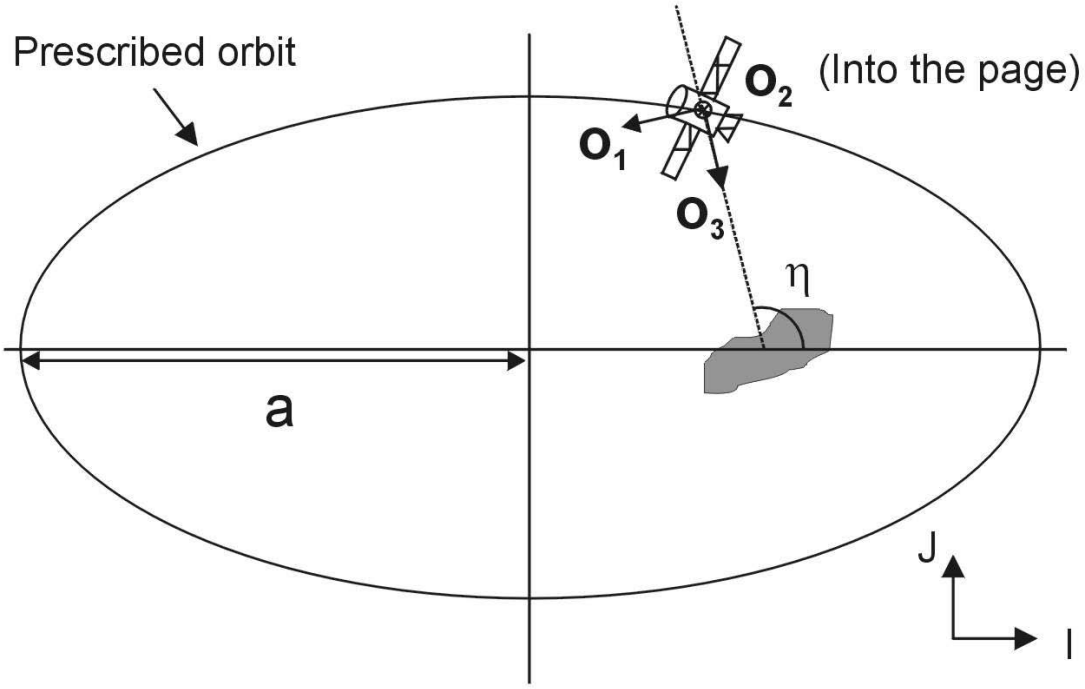


Figure 1. Geometry of the system

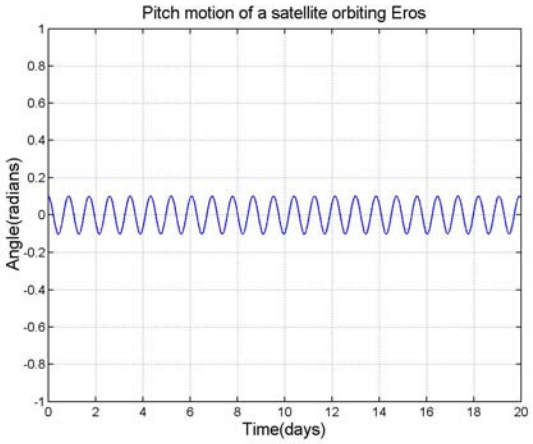


**Figure 2. Pitch motion of a satellite orbiting Eros,** $R_c$=50 km, $k_2$=1/3

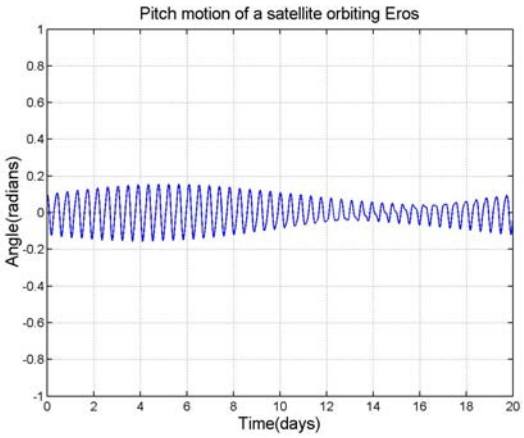


**Figure 3. Pitch motion of a satellite orbiting Eros,** $R_c$=32 km, $k_2$=1/3

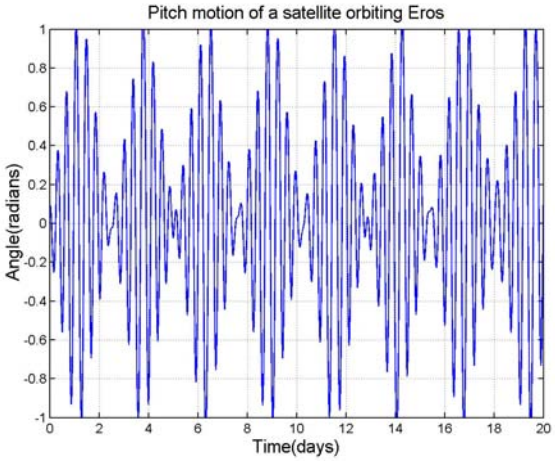


**Figure 4. Pitch motion of a satellite orbiting Eros,**
$R_c$=26 km, $k_2$=1/3

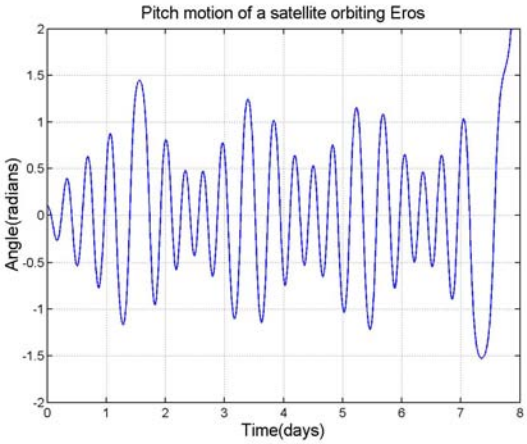


**Figure 5. Pitch motion of a satellite orbiting Eros,**
$R_c$=25.3 km, $k_2$=1/3

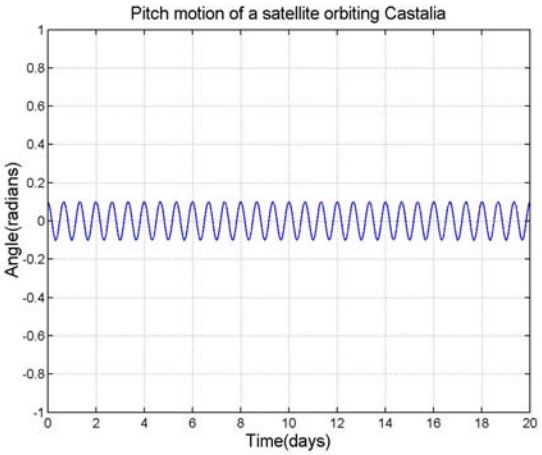


**Figure 6. Pitch motion of a satellite orbiting Castalia**
$R_c$= 2 km, $k_2$=1/3

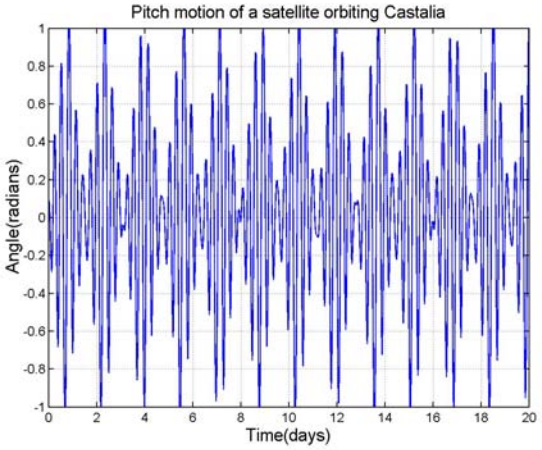


**Figure 7. Pitch motion of a satellite orbiting Castalia,**
$R_c$=1.05 km, $k_2$=1/3

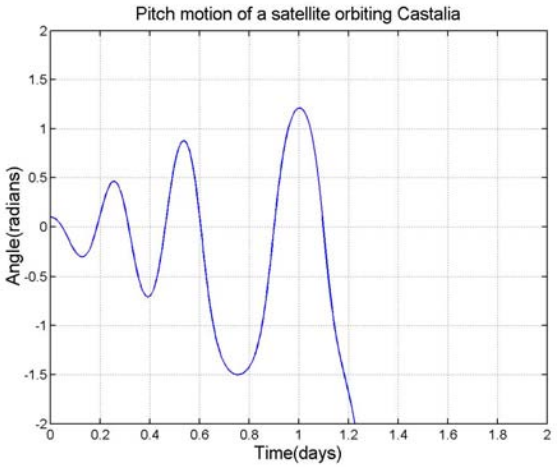


**Figure 8. Pitch motion of a satellite orbiting Castalia,**
$R_c$=1.03 km, $k_2$=1/3

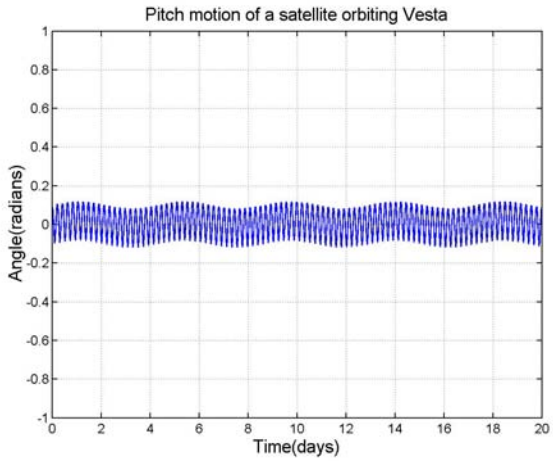


**Figure 9. Pitch motion of a satellite orbiting Vesta,**
$R_c$=500 km, $k_2$=1/3

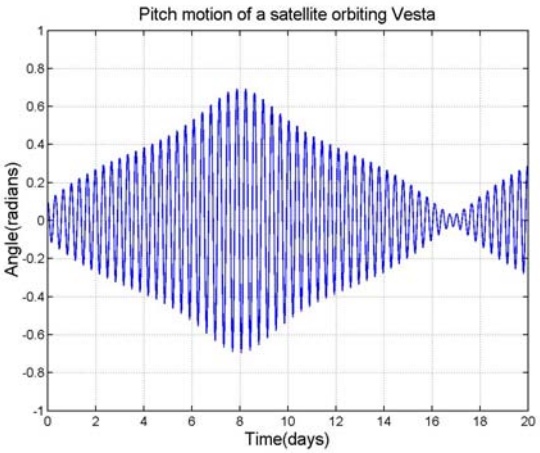


**Figure 10. Pitch motion of a satellite orbiting Vesta,**
$R_c$=661 km, $k_2$=1/3

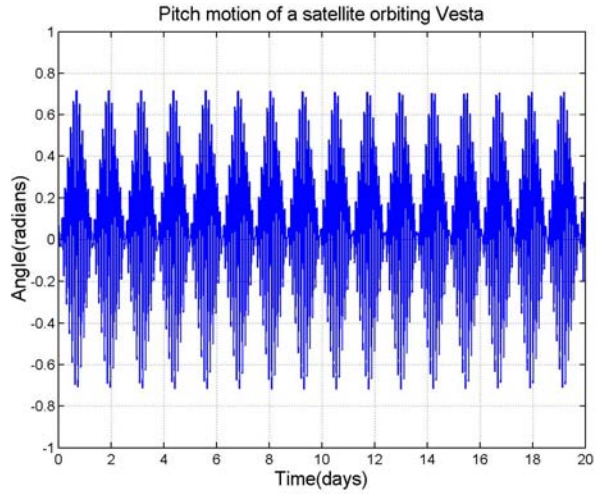


**Figure 11. Pitch motion of a satellite orbiting Vesta,**
$R_c$=312 km, $k_2$=1/3